MHd Pulsatile Flow of an Oldroyd Fluid in a Channel of Porous Medium

S. Sreenadh, E. Sudhakara, and J. Prakash

***Abstract*—** Hydromagnetic pulsatile flow of an Oldroyd fluid in a channel of porous medium is investigated. The flow in the channel is bounded by rigid plates and is driven by an unsteady pressure gradient. The lower and upper plates are maintained at uniform temperatures T_0 and T_1 ($>T_0$) respectively. A uniform magnetic field is imposed along the direction normal to the flow. The expressions for the velocity field and the temperature distribution are obtained. The rate of heat transfer at the plates has also been calculated. We find that the increase in the frequency parameter R_* gives rise to decrease in the velocity of the Oldroyd fluid in the channel. It is observed that the velocity decreases with increasing H_1(which is the square root of sum of the squares of the Hartmann number and the permeability parameter). It is also observed that the temperature increases with the increase in the Prandtl number.

***Keywords*—** Heat transfer, MHD Pulsatile flow, Oldroyd fluid, Porous medium,

I. Introduction

THE study of MHD pulsatile flow of an Oldroyd fluid in a channel or porous pipe has recently become the object of scientific research because of its importance in biological applications in relation to haemodynamics and in industrial applications in relation to heat exchange efficiency. Pulsatile flow is composed of a steady component and a superimposed periodical time varying component called oscillation. Oscillating flow itself is a special pulsatile flow, which is governed by an oscillation only with a zero steady flow component. Pulsatile flow is frequently encountered with captivating applications in natural systems (circulatory system, respiratory system, vascular diseases) as well as engineering systems (reciprocating pumps, IC engines, pulse combustors). Other applications of pulsatile flows arise in the uretral transport, artherosclerosis, interaction with peristaltic flows, flows in curved arteries, cerebral hydrodynamics etc.

Rockwell et al. [1] presented an excellent study discussing pulsatile flow in viscoelastic blood vessels. Chaturani and Upadhya [2] used a couple stress fluid model to study the pulsatile flow in tubes. The leakage to peripheral vessels from pulsatile flow in a principal vessel was discussed by Chadwick [3]. An excellent computational study of pulsatile flow dwelling on nonlinear flow aspects was presented by Hung [4]. Chaturani and Palanisamy [5] studied the effects of periodic body acceleration on the pulsatile flow of blood using a casson model. Pedersen et al. [6] also studied experimentally a variety of pulsatile flows. Other non-Newtonian pulsatile flow studies include those by Sadeghipour and Hajari [7]. An alternative constitutive model for blood rheology was described by Yeleswarupu [8] who generalized the Oldroyd-B flow model with experimental correlation to flow data. Recent rheological biofluid dynamics studies include the models presented by Usha and Prema [9] who employed a particle-fluid suspension model of blood to study the pulsatile flow under periodic body acceleration in a circular conduit.

More recently Eldabe et al. [10] studied the pulsatile hydromagnetic flow of an Eyring-Powell fluid in a parallel-plate channel with couple stress effects. They obtained finite difference solutions for the momentum equation and showed that couple stresses decreases flow velocity. For constant time the velocity was also shown to decrease with increasing pulsation pressure gradient; magnetic parameter was also found to depress velocity for a constant Reynolds number. Vajravelu et al. [11] have analyzed the pulsatile flow between permeable beds. Their study indicated that the maximum velocity is attained between the permeable beds and gradually the velocity decreases towards the upper permeable bed.

A detailed study of non-Newtonian blood flow in small diameter vessels has been presented by Scott [12]. Ogulu et al. [13] have modeled pulsatile blood flow within a homogeneous porous bed in the presence of a uniform magnetic field with time-dependent suction. Srinivas et al. [14] studied on pulsatile hydromagnetic flow of an Oldroyd fluid with heat transfer. Avinash et al. [15] have analyzed pulsatile flow of a viscous stratified fluid of variable viscosity between permeable beds.

In this paper, MHD pulsatile flow of an Oldroyd fluid in a channel of porous medium is considered. The fluid is driven by an unsteady pressure gradient. A uniform magnetic field is applied perpendicular to the channel. Expressions for the velocity and temperature are obtained analytically and numerical solutions are discussed with graphical representation.

S. Sreenadh is with the Sri Venkateswara University, Tirupati-517502 INDIA (e-mail: profsreenadh@gmail.com).

E. Sudhakara, is with the Sri Venkateswara University, Tirupati-517502 INDIA (e-mail: sudhakare1983@gmail.com).

J. Prakash is with the Department of Mathematics, University of Botswana, Private Bag 0022, Gaborone, BOTSWANA (corresponding author's phone:0267 355 2949; e-mail: prakashj@mopipi.ub.bw).

II. Mathematical Formulation

We consider the pulsatile flow of a viscoelastic fluid between two infinitely long parallel plates, at a distance h apart, which is driven by the unsteady pressure gradient.

$$-\frac{1}{\rho}\frac{\partial p}{\partial x} = A\left\{1+\varepsilon \exp(i\omega t)\right\} \tag{1}$$

Where ρ is the density of the fluid, p is isotropic pressure, A is a known constant, ε is a suitably chosen positive quantity and ω is the frequency. Let the x-axis be along one plate and y-axis normal to it. It is assumed that the motion is slow so that all second order quantities may be neglected. A uniform magnetic field is imposed along the direction normal to the flow. In the analysis, we assume that the induced magnetic field is negligible.

This study is based upon the Oldroyd model of a viscoelastic fluid and the properties of such a fluid are specified by three constants η_0, of the dimension of viscosity and λ_1, λ_2 are the relaxation and retardation times respectively. The equations of the state relating to stress tensor p_{ik} and the rate of strain tensor $e_{ik} = \frac{1}{2}\left(u_{i,k} + u_{k,i}\right)$ of such fluids are of the form

$$p_{ik} = p'_{ik} - p\delta_{ik} \tag{2}$$

$$\left(1+\lambda_1\frac{\partial}{\partial t}\right)p'_{ik} = 2\eta_0\left(1+\lambda_2\frac{\partial}{\partial t}\right)e_{ik} \tag{3}$$

Where p_{ik} is the part of the stress tensor related to the change of the shape of a material element and δ_{ik} is Kronecker delta. The liquid ($e_{ii} = 0$) described by the above model behaves as a viscous liquid if $\eta_0 > 0$ and $\lambda_1 = \lambda_2$. The equations of motion combined with constitutive equations of the hydromagnetic viscoelastic fluid through a porous medium are given by

$$\left(1+\lambda_1\frac{\partial}{\partial t}\right)\frac{\partial u}{\partial t} = -\frac{1}{\rho}\left(1+\lambda_1\frac{\partial}{\partial t}\right)\frac{\partial p}{\partial x} + \upsilon\left(1+\lambda_2\frac{\partial}{\partial t}\right)\frac{\partial^2 u}{\partial y^2} - \left(1+\lambda_1\frac{\partial}{\partial t}\right)\left(\frac{\sigma_e B^2{}_e}{\rho} + \frac{\upsilon}{k}\right)u \tag{4}$$

$$0 = -\frac{1}{\rho}\left(1+\lambda_1\frac{\partial}{\partial t}\right)\frac{\partial p}{\partial y} \tag{5}$$

The energy equation is

$$\rho c_p\frac{\partial T}{\partial t} = \chi\frac{\partial^2 T}{\partial y^2} + \mu\left(\frac{\partial u}{\partial y}\right)^2 \tag{6}$$

The boundary conditions are

$$u = 0,\ T = T_0 \text{ at } y = 0 \tag{7}$$

$$u = 0,\ T = T_1 \text{ at } y = h \tag{8}$$

where u is the velocity component in x-direction, σ_e is electrical conductivity, ν is coefficient of kinematic viscosity, μ is the coefficient of dynamitic viscosity, T_0 and T_1 are the temperatures maintained at uniform temperatures at the plate $y = 0$ and $y = h$ respectively.

III. Non-Imensionalization Of The Flow Quantities

We introduce the following non-dimensional quantities

$$\eta = \frac{y}{n}, H^2 = \frac{h^2\sigma_e B_0{}^2}{\mu},\ R_*^2 = \frac{\omega h^2}{\nu}, \nu = \frac{\mu}{\rho}$$

$$\beta^2 = \frac{1+iF_1}{1+iF_1F_2}, F_1 = \lambda_1\omega, F_2 = \frac{\lambda_2}{\lambda_1}(<1),$$

$$\beta_1{}^2 = \beta^2(H^2 + iR_*{}^2), H_1{}^2 = H^2 + \sigma^2,\ \theta = \frac{T-T_0}{T_1-T_0},$$

$$u* = \frac{u}{\left(\frac{Ah^2}{\nu}\right)}, \tau = \omega t \tag{9}$$

Where B_0 is an imposed uniform magnetic field. It can be noted that the results for viscous fluid correspond to the case $\lambda_2 = \lambda_1$, i. e $F_2 = 1$ independent of the values of F_1.

Substituting (9) in (4) and equating the harmonic terms, retaining coefficients of $\varepsilon e^{i\tau}$, the corresponding equations become

$$\frac{\partial^2 u_0}{\partial\eta^2} - H_1^2 u_0 = -1 \tag{10}$$

$$\frac{\partial^2 u_1}{\partial\eta^2} - \beta_1^2 u_1 = -1 \tag{11}$$

Where u_i is velocity vector. Using (9), the energy equation (6) becomes

$$R_*{}^2\frac{\partial\theta}{\partial t} = \frac{1}{Pr}\left(\frac{\partial^2\theta}{\partial\eta^2}\right) + Ec\left(\frac{\partial u^*}{\partial\eta}\right)^2 \tag{12}$$

Where $Pr = \frac{\mu C_p}{\chi}$ and $Ec = \frac{A^2h^4}{\nu^2 C_p\left(T_1 - T_0\right)}$. P_r and E_c represent Prandtl and Eckert numbers respectively, χ is thermal conductivity and C_p is specific heat.

The corresponding boundary conditions are

$$u = 0,\quad \theta = 0 \text{ at } \eta = 0 \tag{13}$$

$$u = 0,\quad \theta = 1 \text{ at } \eta = 1 \tag{14}$$

IV. Solution Of The Problem

The solution of equations (10) and (11) has the form

$$u = u_0 + \varepsilon u_1 e^{i\tau}, \qquad \tau = \omega t \tag{15}$$

Where

$$u_0 = \frac{1}{H_1^2}\left\{1 - \frac{\sin H_1(1-\eta) + \sinh H_1\eta}{\sinh H_1}\right\} \tag{16}$$

$$u_1 = \frac{1}{\beta_1^2}\left\{1 - \frac{\sin \beta_1(1-\eta) + \sinh \beta_1\eta}{\sinh \beta_1}\right\} \tag{17}$$

In view of (15), the temperature θ can be assumed in the form

$$\theta(\eta, t) = \theta_0(\eta) + \omega F(\eta) e^{i\tau} + \varepsilon^2 G_1(\eta) e^{2i\tau} \tag{18}$$

Substituting (18) and u* in (12), equating the harmonic terms, retaining coefficients of ε^2 and solving the corresponding equations for θ_0, F (η) and G_1 (η) with the help of (13) and (14), we obtain

$$\theta_0(\eta) = \frac{-P_r E_c}{8H_1^2 \sinh^2 H_1}\left\{\begin{array}{l} 4\eta^2 + \dfrac{\cosh 2H_1(1-\eta)}{H_1^2} + \\ \dfrac{\cosh 2H_1\eta}{H_1^2} - 4\eta^2 \cosh H_1 - \\ \dfrac{2\cosh H_1(1-2\eta)}{H_1^2} \end{array}\right\} + C_1\eta + C_2 \tag{19}$$

$$F(\eta) = C_3 \sinh A\eta + C_4 \cosh A\eta - \frac{E_c P_r}{\beta_1 H_1 \sinh H_1 \sin \beta_1}\left[\begin{array}{l} \dfrac{1}{A_1^2 - A^2}\left\{\begin{array}{l}\cosh A_1(1-\eta) - \cosh(H_1 - A_1\eta) - \\ \cosh(\beta_1 - A_1\eta) + \cosh A_1\eta\end{array}\right\} + \\ \dfrac{1}{A_2^2 - A^2}\left\{\begin{array}{l}\cosh A_2(1-\eta) - \cosh(H_1 - A_2\eta) - \\ \cosh(\beta_1 - A_2\eta) + \cosh A_2\eta\end{array}\right\}\end{array}\right] \tag{20}$$

$$G(\eta) = C_5 \sinh B\eta + C_6 \cosh B\eta - \frac{E_c P_r}{2\beta_1^2 \sinh^2 \beta_1}\left[\begin{array}{l} \dfrac{\cosh B_1\eta}{B_1^2 - B^2}\left(1 + \cosh B_1 - 2\cosh \beta_1\right) + \\ \dfrac{\sinh B_1\eta}{B_1^2 - B^2}\left(2\sinh \beta_1 - \sinh B_1\right) + \\ \dfrac{2}{B^2}\left(\cosh \beta_1 - 1\right)\end{array}\right] \tag{21}$$

Where $A_1 = H_1 + \beta_1$, $A_2 = H_1 - \beta_1$

$$C_1 = 1 + \frac{P_r E_c}{8H_1^2 \sinh^2 H_1}\left\{\begin{array}{l} 4 + \dfrac{1}{H_1^2} + \dfrac{\cosh 2H_1}{H_1^2} - \\ 4\cosh H_1 - \dfrac{2\cosh H_1}{H_1^2}\end{array}\right\} - C_2$$

$$C_2 = \frac{P_r E_c}{8H_1^2 \sinh^2 H_1}\left\{-\frac{2\cosh H_1}{H_1^2} + \frac{\cosh 2H_1}{H_1^2} + \frac{1}{H_1^2}\right\}$$

$$K_1 = \frac{E_c P_r}{\beta_1 H_1 \sinh H_1 \sinh \beta_1}\left[\begin{array}{l} \dfrac{1}{A_1^2 - A^2}\left(\begin{array}{l}\cosh A_1 - \cosh H_1 \\ -\cosh \beta_1 + 1\end{array}\right) + \\ \dfrac{1}{A_2^2 - A^2}\left(\begin{array}{l}\cosh A_2 - \cosh H_1 \\ -\cosh \beta_1 + 1\end{array}\right)\end{array}\right]$$

$$K_2 = \frac{E_c P_r}{\beta_1 H_1 \sinh H_1 \sinh \beta_1}\left[\begin{array}{l} \dfrac{1}{A_1^2 - A^2}\left\{\begin{array}{l}1 - \cosh(H_1 - A_1) \\ -\cosh(\beta_1 - A_1) \\ +\cosh A_1\end{array}\right\} \\ + \dfrac{1}{A_2^2 - A^2}\left\{\begin{array}{l}1 - \cosh(H_1 - A_2) \\ -\cosh(\beta_1 - A_2) \\ +\cosh A_2\end{array}\right\}\end{array}\right]$$

$$C_4 = K_1, C_3 = \frac{K_2}{\sinh A} - K_1 \coth A,$$

$$K_3 = \frac{E_c P_r}{2\beta_1^2 \sinh^2 \beta_1}\left[\begin{array}{l} \dfrac{1}{B_1^2 - B^2}\{1 + \cosh B_1 - 2\cosh \beta_1\} \\ + \dfrac{2}{B^2}\{\cosh \beta_1 - 1\}\end{array}\right]$$

$$K_4 = \frac{E_c P_r}{2\beta_1^2 \sinh^2 \beta_1}\left[\begin{array}{l} \dfrac{\cosh B_1}{B_1^2 - B^2}\{1 + \cosh B_1 - 2\cosh \beta_1\} \\ + \dfrac{\sinh B_1}{B_1^2 - B^2}\{2\sinh \beta_1 - \sinh B_1\} \\ + \dfrac{2}{B^2}\{\cosh \beta_1 - 1\}\end{array}\right]$$

$$C_6 = K_3, C_5 = \frac{K_4}{\sinh B} - K_3 \coth B, B = R_* \sqrt{2i \Pr}, B_1 = 2\beta_1$$

V. Numerical Results And Conclusions

The variation of velocity with η is calculated, from equation (15) for different values of ωt and is shown in Figures 1 to 3 for fixed F_1, F_2, σ, β_1, ε and H. We observe that the velocity decreases with increasing ωt. We also find that the increase in R_* gives rise to decrease in the velocity of the Oldroyd fluid in the channel.

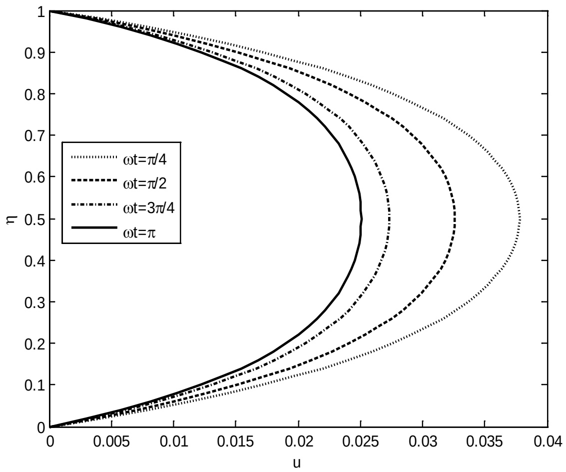

FIG. 1 Velocity distribution for various values of ωt for fixed F_1=0.2, F_2=0.8, σ=5, β_1=0.5, R_*=1, ε=0.1and H=3.

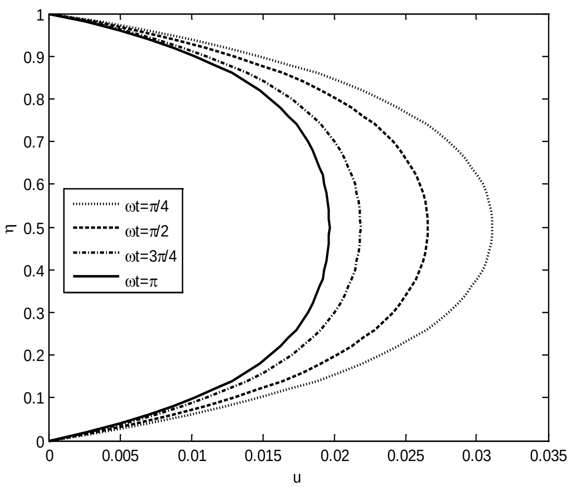

FIG. 2 Velocity distribution for various values of ωt for fixed F1=0.2, F_2=0.8, σ=5, β_1=0.5, R_*=2, ε=0.1 and H=3.

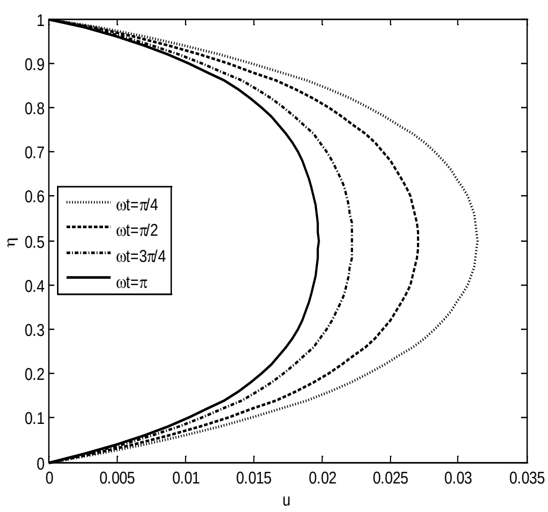

FIG. 3 Velocity distribution for various values of ωt for fixed F_1=0.2, F_2=0.8, β_1=0.5, R_*=3, ε=0.1 and H=3.

The variation of velocity with η is calculated for different values of H, σ and β_1 is shown in Figures 4 to 6 for fixed F_1, F_2, R_*, ε and ωt. We observe that the velocity decreases with increasing H or σ or β_1.

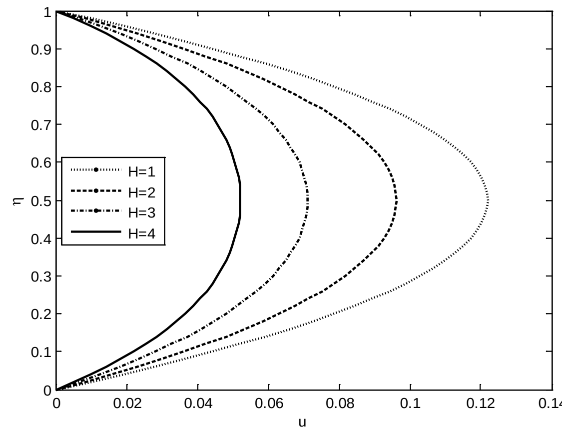

FIG. 4 Velocity distribution for various values of H for fixed F_1=0.2, F_2=0.8, β_1=0.5, σ=0, R_*=1, ε=0.1 and $\omega t = \pi / 4$.

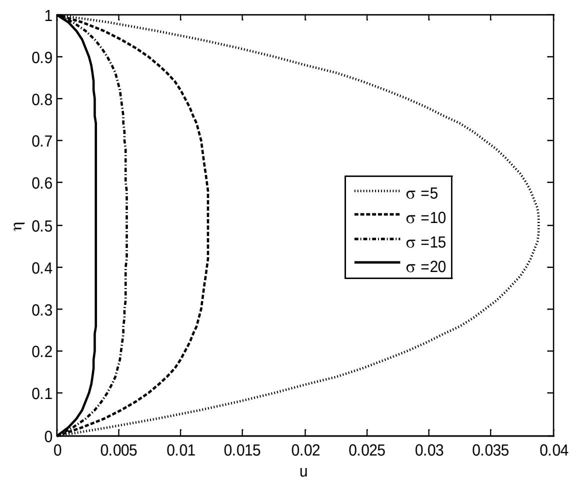

FIG. 5 Velocity distribution for various values of σ for fixed F_1=0.2, F_2=0.8, β_1=0.5, H=0, R_*=1, ε=0.1 and $\omega t = \pi / 4$.

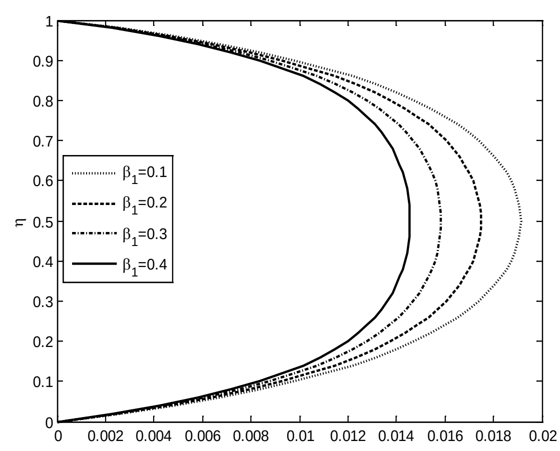

FIG. 6 Velocity distribution for various values of β_1 for fixed F_1=0.2, F_2=0.8, σ=5, H=8, R_*=1, ε=0.1 and $\omega t = \pi / 4$.

From the equation (18), we have calculated the temperature as a function of η, for fixed F_1, F_2, σ, H, R_*, ε, β_1, Ec and ωt and for different values of Pr and is shown in Figure7. We observe that the temperature increases with the increase in Pr. The variation of temperature is evaluated as a function of η, for fixed F_1, F_2, Pr, R_*, ε, β_1, Ec and ωt and for different values of σ and H and is shown in Figures 8 and 9. It is observed that the temperature increases with the decreasing H or σ.

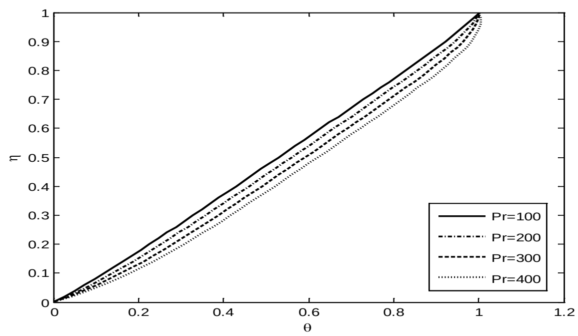

FIG. 7 Temperature distribution for various values of Pr for fixed F_1=0.2, F_2=0.8, σ=5, β_1=0.5, R_*=0.1, ε=0.1,H=3, Ec=1 and $\omega t = \pi / 4$.

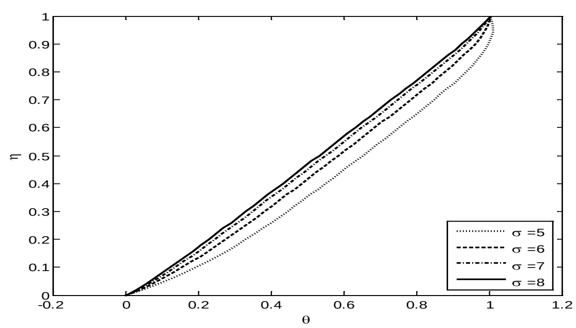

FIG. 8 Temperature distribution for various values of σ for fixed F_1=0.2, F_2=0.8, β_1=0.5, Pr=300, R_*=0.1, ε=0.1, H=0, Ec=1 and $\omega t = \pi / 4$.

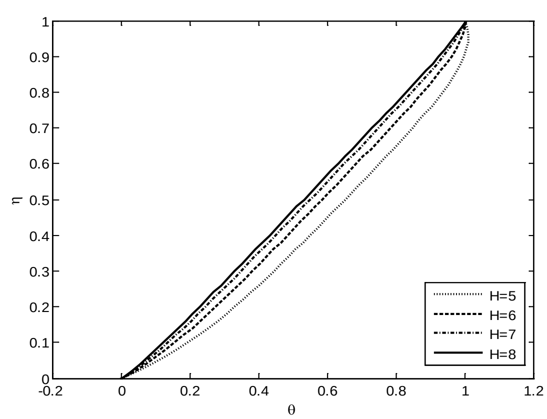

FIG. 9 Temperature distribution for various values of H for fixed F_1=0.2, F_2=0.8, σ=0, β_1=0.5, R_*=0.1, ε=0.1, Pr=300, Ec=1 and $\omega t = \pi / 4$.

The effect of changing the Hartmann number (for fixed Ec) and changing Eckert number (for fixed H_1) are shown in Tables I and II. Table I shows that the rate of heat transfer from the lower plate decreases with increasing Hartmann number, whereas it increases in the upper plate. We observe from Table II that the rate of heat transfer from the lower plate increases with Ec while at the upper plate, the heat flows from the fluid to the plate even if $T_1 > T_0$.

TABLE I

EC = 1, PR = 100, R_* = 1

	$H_1 = 0$	**$H_1 = 1$**	**$H_1 = 2$**	**$H_1 = 3$**
$Nu_1=(\theta_0^1)_{\eta=0}$	17.6518	14.7787	9.5485	5.69695
$Nu_2=(\theta_0^1)_{\eta=1}$	-15.6518	-12.7787	-7.5405	-3.6969

TABLE II

PR = 10, H1 = 1.5, R* = 1

	Ec = 1	**Ec = 2**	**Ec = 3**	**Ec = 5**
$Nu_1=(\theta_0^1)_{\eta=0}$	2.1123	3.2247	4.3371	6.5618
$Nu_2=(\theta_0^1)_{\eta=1}$	-0.11235	-1.22471	-2.33706	-4.56177

The effect of changing elastic parameters and changing H_1 (for fixed Ec) and changing R_* (for fixed Ec) and changing Ec (for fixed H_1), on the values of the amplitude and phase of the rate of heat transfer is shown in Tables III, IV and V. In Table III, it is observed for a viscoelastic an Oldroyd fluid, the increase in Hartmann number decreases the amplitude of heat transfer at both the plates. It may be observed from Table IV that at the lower plate there is a phase lag at higher frequency, but at the upper plate there is a phase lead. We also find that at both the plates the amplitude decreases uniformly with frequency for fixed Ec. It can be noticed from Table V for fixed R_* that the amplitude increases uniformly with Ec at both the walls. The increase of the Eckert number Ec increases the amplitude of heat transfer at the plates for the viscoelastic fluid, while the phase at the plates remains unaffected by the increase of Ec.

TABLE III

PR = 200, R* = 10, F1 = 0.1, F2 = 0.5, EC = 3

H_1	$\lvert D_0 \rvert$	$\lvert D_1 \rvert$	tan α_0	tan α_1
0	0.261855	0.0231703	-29.0306	12.9313
0.2	0.260977	0.0231044	-28.8304	12.8729
0.4	0.258385	0.0229097	-28.2463	12.7017

TABLE IV

PR = 200, F1 = 0.1, F2 = 0.4, H1 = 0.3, EC = 5.

R_*	$\lvert D_0 \rvert$	$\lvert D_1 \rvert$	tan α_0	tan α_1
5	2.73881	0.265488	-61.0054	5.35171
10	0.649884	0.0575502	-25.151	14.5618
15	0.29009	0.0244279	-29.1139	33.4444

TABLE V

PR = 200, F1 = 0.1, F2 = 0.5, H1 = 0.2, EC = 5.

Ec	$\left\|D_0\right\|$	$\left\|D_1\right\|$	tan α_0	tan α_1
5	2.74875	0.266414	-84.1425	5.12845
10	5.49751	0.532828	-84.1425	5.12845
15	8.24626	0.799242	-84.1425	5.12845

ACKNOWLEDGMENT

One of us (S. Sreenadh) would like to thank to University Grants Commission (UGC), Government of India for providing financial support through the Major Research Project to undertake this work.

REFERENCES

[1] Rockwell, R.L., Anliker, M. and Elsner, J., Model studies of the pressure and flow pulses in a viscoelastic arterial conduit. *J. Franklin Institute*., Vol. **297**, pp. 405-427, 1974. http://dx.doi.org/10.1016/0016-0032(74)90042-8

[2] Chaturani, P. and Upadhya, V.S., Pulsatile flow of a couple stress fluid through circular tubes with applications to blood flow. *Biorheolog*y., Vol.**15**, pp. 193-201.1978.

[3] Chadwick, R.S., Pulse wave propagation in an artery with leakage into small side branches. Proc. *National Academy of Sciences*, USA, Vol. **82**, pp.5237-5241, 1985 http://dx.doi.org/10.1073/pnas.82.16.5237

[4] Hung, T. K., Nonlinear Characteristics of Pulsatile Flows, Proceedings of the 5th ICMMB, Bolognia, Italy, pp. 87-89, 1986.

[5] Chaturani, P. and Palanisamy, V., Casson fluid model for pulsatile flow of blood under periodic body acceleration. *Biorheology*., Vol. **27(5)**, pp. 619-630. 1990.

[6] Pedersen, E.M., Sung, H.W., Burlson, A.C. and Yoganathan, A.P., Two-dimensional velocity measurements in a pulsatile flow model of the abdominal aorta simulating different hemodynamic conditions. *J. Biomechanics*, Vol. **26**, pp.1237-1247, 1993. http://dx.doi.org/10.1016/0021-9290(93)90071-L

[7] Sadeghipour, M.S. and Hajari, B., Pulsatile blood flow in deformable vessels-non- Newtonian behaviour, Proc. *ASME/AICHEME/ASCE Summer Bioengineering Conference, BED-*,Vol. **29**, pp. 345-346, 1995.

[8] Yeleswarupu, K.K. Evaluation of continuum models for characterizing the constitutive behaviour of blood. PhD Dissertation, Mechanical Engineering, University of Pittsburgh, Pennsylvania, USA, 1996

[9] Usha, R. and Prema, K., Pulsatile flow of particle-fluid suspension model of blood under periodic body acceleration. *ZAMP*, Vol. **50(2)**, pp. 175-192, 1999. http://dx.doi.org/10.1007/s000330050145

[10] Eldabe, N.T.M., Hassan, A.A. and Mohamed, A.A., Effect of couple stresses on the MHD Non-Newtonian Unsteady Flow between two parallel porous plates, *Z. Naturforsh.*, Vol. **58**, pp. 204-210, 2003

[11] Vajravelu, K., Ramesh Babu, V., Sreenadh, S. and Arunachalam, P.V., Pulsatile flow between permeable beds, *Int. J. Non-Linear Mech*. Vol. **38**, 999-1005, 2003. http://dx.doi.org/10.1016/S0020-7462(02)00045-8

[12] Scott, M, The modeling of blood rheology in small vessels, PhD Thesis, Applied Mathematics, University of Waterloo, Ontario, Canada. 2005.

[13] Ogulu, A. and Amos, E., Modeling pulsatile blood flow within a homogeneous porous bed in the presence of a uniform magnetic field and time-dependent suction, *Int. Commun. Heat and Mass Transfer,* Vol. **34,** pp. 989-995, 2007 http://dx.doi.org/10.1016/j.icheatmasstransfer.2007.05.012

[14] Srinivas, S., Malathy, T. and Sachdev, P.L., On pulsatile hydromagnetic flow of an Oldroyd fluid with heat transfer, *Engng. Trans.*Vol **55 (1),** pp.79-94, 2007

[15] Avinash, K., Ananda Rao, J., Sreenadh, S. and Ravikumar, Y.V.K., Pulsatile flow of a viscous stratified fluid of variable viscosity between permeable beds, *Journal of Porous Media*, Vol. **14 (12),** pp. 1115-1124, 2011. http://dx.doi.org/10.1615/JPorMedia.v14.i12.60